ACS OMEGA

http://pubs.acs.org/journal/acsodf

Article

Development of a Smart Scaffold for Sequential Cancer Chemotherapy and Tissue Engineering

Poulomi Sengupta, Vinay Agrawal, and Bhagavatula L. V. Prasad*

Cite This: *ACS Omega* 2020, 5, 20724−20733

Read Online

ACCESS | Metrics & More | Article Recommendations | Supporting Information

ABSTRACT: The fabrication of a dual-functional drug-containing porous polymeric scaffold by layer-by-layer surface modification involving citrate-stabilized gold nanoparticles and cisplatin molecules is being reported. These scaffolds were characterized by electron microscopy and X-ray photoelectron spectroscopy. The capability of the scaffolds to release hydrated cisplatin in a slow and sustained manner over two days is established. Most importantly, the scaffolds turn nontoxic and cell-friendly after drug release, thus allowing the noncancerous fibroblast cells to adhere and proliferate (from 5000 cells to 16,000 cells in 6 days), becoming a potential solution toward an effective drug-carrying scaffold for volume-filling applications. The scaffold-mediated cancer cell killing and fibroblast cell proliferation were confirmed by fluorescence microscopy imaging, flow cytometry, and cell proliferation assays. We surmise that such a dual-purpose (drug-delivery and volume-filler) scaffold could help avoid the multiple surgical interventions needed for tumor surgery and cosmetic corrections. To the best of our knowledge, this is the first example of scaffolds with such a dual functionality which gets manifested in a sequential manner.

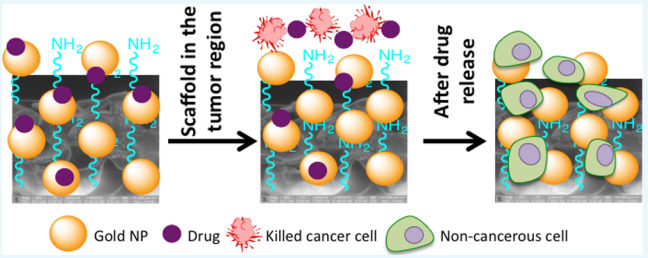

INTRODUCTION

Treatment of cancer involving solid tumors (especially oral cavity cancer) entails three major steps:[1] (1) removal of the tumor by surgery, (2) chemotherapy/radiotherapy or combination, and (3) reconstructive surgery. Here, the surgical intervention (removal of the tumor), the first line of therapy,[2] is generally followed by a planned exposure to chemotherapy, radiation therapy, targeted chemotherapy[1] (for the treatment of the leftover cancerous tissue/cells), or a combination of the above over a certain period. Finally, a corrective surgery (also known as the "limb salvage surgery") may be carried out to offset the deformities caused by the first surgery.[3] Depending upon the size and stage of the tumor, this (corrective surgery) may be performed immediately after the removal of the tumor or after the chemotherapy regime is completed.[4]

Among the three steps listed above, while the surgical intervention has been more or less mastered, the other two are fraught with few issues that need to be addressed. For example, depending on the severity of the cancerous growth, the chemotherapy/radiation therapy routine is implemented at predetermined time intervals over a period. In this regime, highly toxic chemotherapeutic drugs (dosage, frequency, and intervals are predecided by a group of oncologists) are systemically administered to the patients. In addition to the inconvenience caused by the repetitive hospital visits, the systemic administration of the highly toxic drugs leads to many side effects (rapid deterioration of health, weight, hair loss, vomiting, and frequent hospitalization) causing great trauma to the patient. This is the first and major problem that needs to be addressed. Subsequent to this, the patient may need/want to undergo the corrective cosmetic surgery as mentioned above. This is generally performed using polymeric scaffolds, which act as an extracellular matrix that interacts with the cells leading to the formation of new tissues.[5] For this, the polymer scaffolds should possess proper architecture and mechanical properties in addition to the desired characteristics that support cell adhesion, proliferation, and differentiation. Much research has been done on the topic of polymeric scaffold properties such as surface topographic features (roughness and hydrophilicity) and scaffold microstructures (pore size, porosity, pore interconnectivity, and pore and fiber architectures) that influence the cell−scaffold interactions.[6,7] Among the different options available, scaffolds made with the exceptionally biocompatible and nonbiodegradable high-density polyethylene (HDPE) are still the most preferred ones because of many advantages (e.g., flexibility in the size of pores, high tensile strength, expansion coefficient, enhanced surface area, sturdiness, etc.).[8,9] Unfortunately, HDPE-type polymers have a slower rate of integration with the active tissue which is mainly due to their inherent high hydrophobic-

Received: November 1, 2019
Accepted: May 26, 2020
Published: August 11, 2020

https://dx.doi.org/10.1021/acsomega.9b03694
ACS Omega 2020, 5, 20724−20733

Scheme 1. Preparation of the "Dual-Purpose" Scaffold; (A) Polyethylene Scaffold; (B) Freshly N_2 + H_2 Plasma-Treated Scaffold; (C) Citrate-Capped AuNP-Coated Polyethylene Scaffold; and (D) Aquated Cisplatin-Conjugated Polyethylene Scaffold; The Insets (D1, D2, and D3) Provide Details of the Binding of Cisplatin with Citric Acid Present on the AuNP Surface. Cisplatin Hydration to Aquated Cisplatin (E) is Also Shown

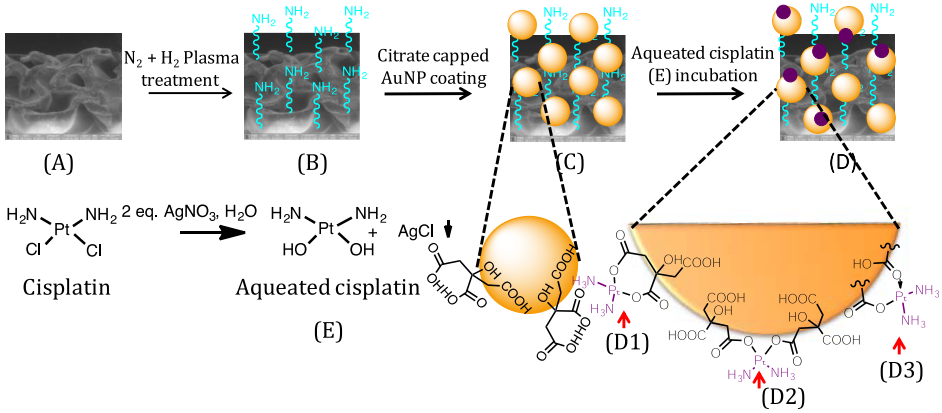

ity.[10−13] Thus, scaffolds made up of such hydrophobic polymers would require a long "healing time". This is the second problem that needs to be dealt with.

One way of addressing the abovementioned two problems is to design and fabricate drug-loaded scaffolds using HDPE-like polymers that can provide "local chemotherapy"[14] for a given time and subsequently become cell-friendly to turn into the usual tissue engineering scaffolds. The drug-loaded scaffolds can be inserted at the region of surgery, and the slow and sustained local release of cytotoxic drugs from the implanted scaffolds over a long period of time would be able to replace the repetitive chemotherapeutic treatment program. Most importantly, in local chemotherapy, as the drugs are exposed to a restricted area (tumorous region only), the toxic side effects associated with the systemic administration of the drug may be prevented. Furthermore, once the drug gets released, the scaffold portrays a proper surface architecture (hydrophilicity and surface chemistry) that will support cell adhesion and proliferation.

Accordingly, in this paper, we report the development of a bifunctional smart HDPE scaffold using a layer-by-layer surface modification technique [involving plasma treatment and citrate-stabilized gold nanoparticle (AuNP) coating].[15,22] These polymeric scaffolds were then decorated with the chemotherapeutic drug cisplatin. Cisplatin is an affordable chemotherapy medication that is widely used in treating most solid tumors including head and neck cancer.[16] At the same time, cisplatin is very toxic to healthy tissue, which invariably leads to terrible side effects.[17,18] To overcome these disadvantages, we have chemically conjugated dihydrated cisplatin analogue to the HDPE surface via the acid−base chemistry involving citric acid groups present on AuNPs. We hypothesized that under in vivo conditions, at tumorous pH, hydrated cisplatin molecules get released (from the scaffold) in a slow and sustained manner. After the drug release, the surface of the biocompatible, nonbiodegradable HDPE scaffold retains the hydrophilic character because of the presence of citrate-capped AuNPs promoting the adhesion and proliferation of noncancerous cells, leading to a healthy tissue formation. Our results indicated that the released hydrated cisplatin was highly effective when tested against the human mouth carcinoma cell line KB under in vitro conditions. To validate that the scaffolds can promote the adherence and proliferation of noncancerous cells post drug release, the same scaffolds were exposed to murine fibroblast cells (L929). Healthy growth of cells over a long time was observed proving the efficacy of the dual-purpose scaffold. We thus propose that a surface-modified, drug-attached HDPE scaffold can serve both the purposes: as a drug delivery system and as an attachment support for tissue regeneration as a part of the postsurgical care of the limb salvage procedure. If translated, this strategy can bring down the level of trauma and tension associated because of a series of surgeries performed on the solid tumor (especially oral cancer)-bearing patients.

RESULTS AND DISCUSSION

The inherent problem of HDPE scaffolds in tissue engineering is their reported slow integration with fresh tissue.[10−12] This is mainly ascribed to their hydrophobic nature. Some of us earlier reported a procedure where with the help of plasma treatment and metallic nanoparticles, this shortcoming could be circumvented.[15,19] We followed a similar strategy[20,21] to design the dual-functional scaffold as part of this study. The specific details of the scaffold preparation are detailed below (Scheme 1). According to this procedure, the three-dimensional (3D) scaffolds [Scheme 1A] were first exposed to the N_2 + H_2 plasma. Immediately after the plasma treatment [Scheme 1B], the scaffolds were immersed in a sol containing citrate-capped AuNPs, which lead to the anchoring of AuNPs onto the scaffolds. After the scaffolds were coated with AuNPs [Scheme 1C], the hydrated cisplatin units were chemically conjugated with the carboxylic acid units (arising from citric acid capping) present on the scaffold's surface using the facile acid−base coupling chemistry [Scheme 1D]. We first characterized, the surface change due to the abovementioned treatments (AuNP-coating and conjugation with hydrated cisplatin) on HDPE scaffolds using UV−visible spectroscopy (please see the Supporting Information section, Figure S3). In both the samples [AuNP-coated (a) and drug-loaded (b)], a typical localized surface plasmon resonance (LSPR) peak for AuNP was observed, which suggests the anchoring of AuNPs on the HDPE surface and also proves that following the chemical treatment during cisplatin conjugation, the AuNP did not fall off. In the case of AuNP-coated HDPE [Figure S3, curve (a), black line], it is seen that the LSPR peak of AuNP appears around 543 nm.[22] This shift (typically AuNP's display LSPR

https://dx.doi.org/10.1021/acsomega.9b03694
ACS Omega 2020, 5, 20724−20733

peak at 520 nm) is ascribed to the aggregation of particles after deposition on the solid HDPE surface. After incubation with 1.0 mg/mL aquated cisplatin solution, the LSPR peak was again seen at 544 nm (Figure S3). Apart from that, a small hump at 580 nm was also observed [Figure S3, curve (b), red line] which we attribute to the interaction of AuNPs with the aquated cisplatin conjugated through a citric acid linker [as shown in Scheme 1D1]. The full width at half-maximum of the peak [curve (a), Figure S3] before drug loading was determined to be 48.5 nm, while the same for the drug-loaded scaffold turned out to be 63.8 nm. This broadening of gold SPR is another indication of a significant change in the surrounding environment of the AuNPs on the scaffold.[22] Thus, UV−visible experiments clearly prove the presence of AuNPs on scaffolds and gave us a hint about the presence of aquated cisplatin. The HDPE surface covered by AuNPs was also subjected to 3D X-ray microtomography imaging (Figure S4). From this, we could see the presence of AuNPs everywhere on the HDPE surface indicating that the plasma treatment was ubiquitous, allowing AuNPs to adhere to the treated surface in a uniform manner. It may also be noted that for 3D X-ray microtomography, in general, the polymeric samples are incubated in KI solution for better contrast. Because AuNPs got anchored to the HDPE surface in a uniform manner in our experiments, we could carry out the imaging without any further treatment as mentioned above. To confirm the presence of platinum on the HDPE surface, the scaffolds after cisplatin conjugation were analyzed by X-ray photoelectron spectroscopy (XPS) (Figure 1). The peaks in

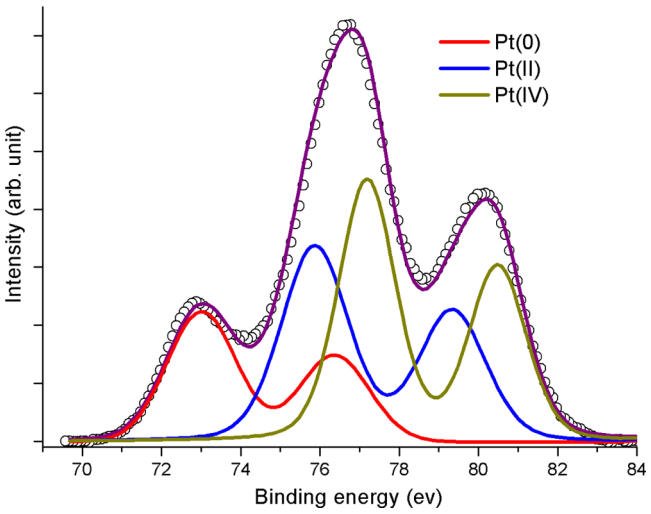

Figure 1. Deconvoluted XPS spectra of the Pt 4f region fitted to different Pt species.

the XPS spectra in the 60−140 eV regions could be fitted to three sets of curves. Among these, the first set of peaks at 65 and 98 eV is attributed to Pt(IV) species, while the ones at 76 and 110 eV and 111 and 139 eV could be ascribed to Pt(II) and Pt(0) species, respectively. Thus, the XPS data indicated that platinum is predominantly present as Pt(IV) and Pt(II) species with a minor component corresponding to Pt(0). In aquated cisplatin, platinum exists as Pt(II). Pt(II) can attach to the citric acid present on the AuNP surface by binding with one citric acid or with two citric acid molecules [Scheme 1D1,D2], respectively, by forming two covalent bonds. Alternatively, it can also bind to one citric acid molecule through one covalent and one coordinate bond [Scheme 1D3]. In all of these cases, Pt(II) is retained on the surface. Among these different Pt species, the amount of Pt(II) and Pt(IV) was found to be significant as determined by the area under the curves. The presence of Pt(IV) on the scaffold may come from the disproportionation reaction of Pt(II) to Pt(0) and Pt(IV). Fortunately, Pt(IV) is also a prodrug[23,24] which in vivo gets converted to Pt(II) before it acts on nuclear DNA. Pt(IV) also is being widely researched for its ability to work in those patients who have acquired cisplatin resistance.[25] Therefore, having Pt(IV) will be an advantage, as both Pt(II) and Pt(IV) can act at different time points on cancerous cells having different growth phases and lead to apoptosis. Finally, to determine the amount of total Pt present on the HDPE surface, we carried out the *o*-phenylenediamine assay (Supporting Information sections S3 and S4) which revealed the average loading of active platinum (by absorbance at 706 nm) on each scaffold to be 0.0771 mg. Cisplatin being a very potent drug has a very low IC_{50} value for almost all cell lines (other than cisplatin-resistant ones). For the cell line under study (human oral carcinoma cell line KB), the IC_{50} value is 0.11 μM,[26] and it is clear that the scaffolds are coated with enough cisplatin to meet this requirement. It may also be noted here that although the chemotherapy planned by the oncologists depend on the affected area and stage of cancer, with such a high loading of the drug, the scaffolds synthesized can meet any demand and have a good chance of being translated. The extent of drug-loading on the HDPE scaffolds can depend on the amount of AuNPs coated, which can be controlled by the time of AuNP incubation after plasma treatment. Also, the drug loading can be increased to a great extent by changing the concentration of the aquated cisplatin.

One of the concerns with the surface modification process is the possible loss of the porous interconnected structure of the scaffolds. To show the retention of the scaffold's morphology, despite the scaffold's exposure to various chemicals, we analyzed them by scanning electron microscopy (SEM) after each treatment. The SEM image in Figure 2A at high resolution indicates 70−100 μm size interconnected pores present in the HDPE scaffolds. After $N_2 + H_2$ plasma treatment and citrate gold coating, there was practically no change in the scaffold structure (Figure 2B), which proves there is not much deformation associated with the surface modification technique. From Figure 2C, it is evident that cisplatin-coated HDPE scaffolds' surface morphology is also not much different from that of the AuNP-coated ones. EDAX of the 2(C) sample proved the presence of the cytotoxic drug cisplatin in 1.09 weight percent (Figure 2D). Also, there was no loss of AuNPs, between (C) and (D) (Scheme 1) by visual observation.

After establishing that the cisplatin is clearly anchored onto the AuNP-decorated HDPE scaffolds and that there was no significant structural alteration in the scaffolds, we focused our attention on the release kinetics of the drug. For this, an in vitro release experiment was performed involving phosphate-buffered saline (PBS) (pH 7.4) and spent media (from overgrown KB cells) where % drug released was plotted against time. In this release kinetics experiment (see the Experimental Section for details), the amount of cisplatin released was calculated by reacting with *o*-phenylenediamine using the calibration curve (Supporting Information sections S3 and S4). From the release kinetics experiment (Figure 3), it is observed that in the spent medium (acidic, pH 5.5), a comparatively higher amount of hydrated cisplatin gets released with respect

https://dx.doi.org/10.1021/acsomega.9b03694
ACS Omega 2020, 5, 20724−20733

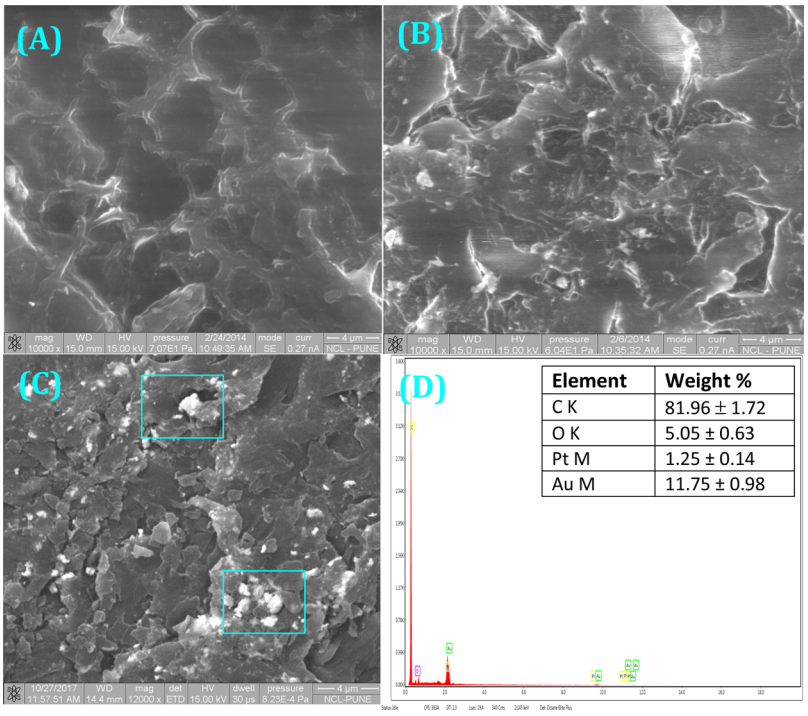

Figure 2. SEM images of the scaffold after different treatments: (A) pristine HDPE scaffolds, (B) AuNP-coated HDPE scaffolds, and (C) AuNP-coated scaffold after incubation with aquated cisplatin. (D) Energy-dispersive system analysis of the sample presented in (C). Data are represented as the mean ± SD of $n = 3$. Two of the detected areas are marked on (C).

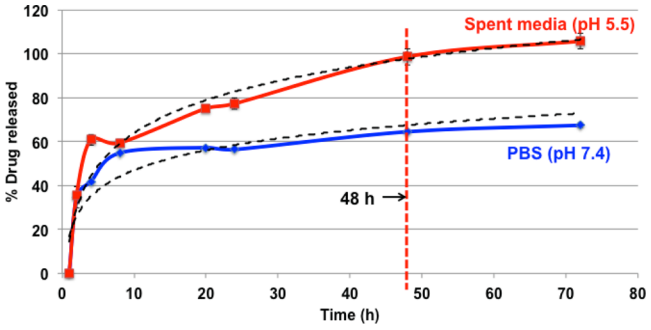

Figure 3. Release profile of cisplatin drug in different environments (data are represented as the mean ± SD of $n = 3$). Optimal time for complete drug release was determined to be 48 h.

to that released in neutral PBS buffer. This may arise due to the faster hydrolysis of the ester-like group present between Pt(II) and citric acid at these lower pH values.[27] We anticipate that in vivo, this property will help to expedite the drug release in the affected (tumorous) region (acidic microenvironment) and be dormant at the vicinity of healthy tissues, thus reducing the side effects of chemotherapy. In addition to the advantages of local chemotherapy, the triggered release will help in managing the negative side effects arising from cytotoxic drugs. The trend of hydrated cisplatin released at specific time points for both acidic (red) and neutral (PBS, blue) solvent (Figure 3) indicates that the release profile is a "burst release" to begin with (within 10 h, almost 60% drug got released), but at the later time points, there is slow and sustained release. From the plot, it is also evident that at 48 h (2 days), almost all the loaded hydrated cisplatin got released from the scaffolds in acidic media. We cross-checked the amount of platinum present, using the previously mentioned cisplatin assay, on the scaffolds which have undergone the release experiment (Supporting Information sections S3 and S4). The findings are plotted in Figure S5 in the Supporting Information. Here, the results indicate that less amount of platinum is present on scaffolds treated with spent media (~2.42 μg) as compared to those treated with PBS alone (~13.63 μg) supporting our abovementioned conclusion that in spent media (lower pH), more cisplatin gets released.

The release pattern of hydrated cisplatin molecules from (D) (Scheme 1) intrigued us to look into the nature of bonding between the AuNP-coated HDPE scaffold and hydrated cisplatin molecules. To know the role of citrate-capped AuNPs deposited on the HDPE scaffold for cisplatin conjugation, both bare HDPE scaffold and AuNP-coated HDPE scaffolds were separately incubated (overnight) in the same stock of 1.0 mg/mL hydrated cisplatin solution (Supporting Information section S5). Upon analyzing the amount of cisplatin present on both the scaffolds, it was found that AuNP-coated scaffolds hold more amount of cisplatin (Figure S6). This could be due to the fact that on HDPE scaffolds decorated with AuNPs, cisplatin is present through covalent bonding, while on pure HDPE scaffolds, only a small quantity of hydrated cisplatin is present because of nonspecific adsorption.

The extent of the drug's effect on cells can be determined by a cell viability assay. We chose the human mouth carcinoma KB cell line which was maintained in 10% fetal bovine serum (FBS)/minimum Eagle's essential medium (MEM). In the assay, we performed a control experiment using an unmodified scaffold, AuNP-coated scaffold, and compared the results with cisplatin-containing scaffolds, along with aquated cisplatin (we used the same amount of cisplatin as was present on the scaffold). The release kinetics experiment presented showed that at 24 h, at least 70% of the drug got released (Figure 3). Based on this, the time point for cell viability was decided to be

https://dx.doi.org/10.1021/acsomega.9b03694
ACS Omega 2020, 5, 20724−20733

48 h. With the resazurin assay, it has been observed that when the cells were incubated with cisplatin-loaded scaffolds, only 60% of cells were viable (Figure 4) by the end of 48 h. In comparison, when exposed to a free drug of equal quantity, only 40% of cells were found viable. This can arise from the easy internalization of free drugs into live cells, in comparison with the polymer-bound drug (via citric acid-capped AuNPs), which has to overcome a release step through bond cleavage by ester bond hydrolysis. Quite gratifyingly, AuNP-coated scaffolds were found to be nontoxic (showing more than 100% cell viability in Figure 4), which is important because according to our proposal, the scaffolds after drug release should be accepting new cells; hence, it should not portray any cytotoxicity. The *P* values were also incorporated in Figure 4, which indicated that the data were significant.

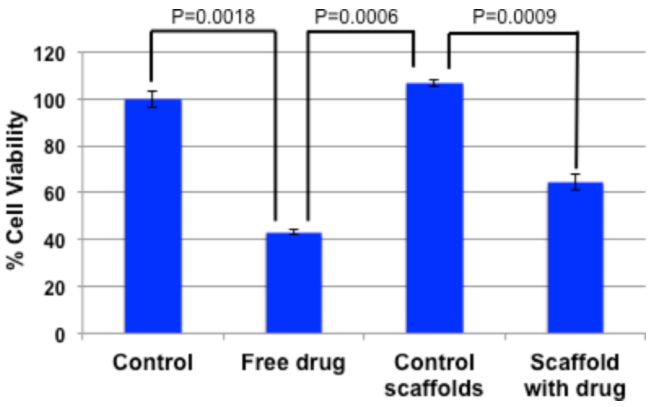

Figure 4. Cell viability assay with KB (human mouth cancer) cells. Quantification of cells via mitochondrial activity using resazurin as an indicator (data are represented as the mean ± SD of $n = 3$).

To validate the presence and quantity of dead and live cells in situ, a live−dead experiment was carried out. The control coverslips containing only cells showed a beautiful array of live cells; not a single dead cell was visible (Figure 5 upper panels). For the AuNP-coated scaffold containing coverslip, most of the cells were live, although few dead cells were also seen (same Figure 5, middle panels). For the cisplatin-carrying scaffold, mostly dead cells populated the coverslips. The fluorescence coming off the different channels also predict the similar trend (Supporting Information, Figure S7). It is worth mentioning here that the ratio between live cells and dead cells is quite similar to that obtained from the cytotoxicity study. Briefly, the amount (number) of cells for both control and gold-coated scaffold containing wells is high, so it is relatively easier to get a trend. However, for drug-loaded scaffold containing wells, because of cisplatin's cytotoxicity, the cells die and get washed away during PBS wash. Therefore, the majority of cells that get washed away is actually dead cells.

The extent/nature of cell death initialized by cisplatin was investigated with the help of flow cytometry, using Annexin-V fluorescein isothiocyanate (FITC) (apoptosis marker), and propidium iodide (PI) (dead cell marker) dyes. To check that cells were not displaying any autofluorescence, cells without any marker were allowed to pass through the analyzer but no signal for red or green fluorescence was observed (Figure 6 top panels). For control cells (without any cisplatin exposure), where both markers were added, no apoptosis or necrosis was in progress, so the cells were completely healthy and did not show any signal for red/green fluorescence (Figure 6 middle panel). Cells, which have got exposed to a cisplatin environment for 24 h, showed a significant signal for early apoptotic and late apoptotic stages (Figure 6 lower panel). A cytotoxic drug such as cisplatin initiates intercalation in the DNA of the nucleus of a live cell and forces the cell to undergo apoptosis. Cells, which have got exposed to a cisplatin environment for 24 h, showed a significant signal for early apoptotic and late apoptotic stages. Similarly, cells, which were exposed to drug-loaded scaffolds, showed 65% early apoptotic and almost 30% late apoptotic cells (Supporting Information, Figure S8). It may also be noted that we chose a 1 day time point for this analysis as many cells were found dead after 2 or later day time points (data not included), and the data points were not enough to identify a trend. The Annexin-V FITC conjugate was also used for imaging purpose, where the extent of phosphatidylserine expression can be visualized and quantified. Figure S9 (Supporting Information) indicates that control cells (without any exposure to the cisplatin scaffold) did not display any green fluorescence. With cisplatin-exposed cells on day 1 (middle panel), several cells showed green fluorescence around the cellular membrane region, which arose from the FITC attached to phosphatidylserine present in the cellular membrane. On day 2 (lower panel), almost all these cells had well-expressed phosphatidylserine along the cellular

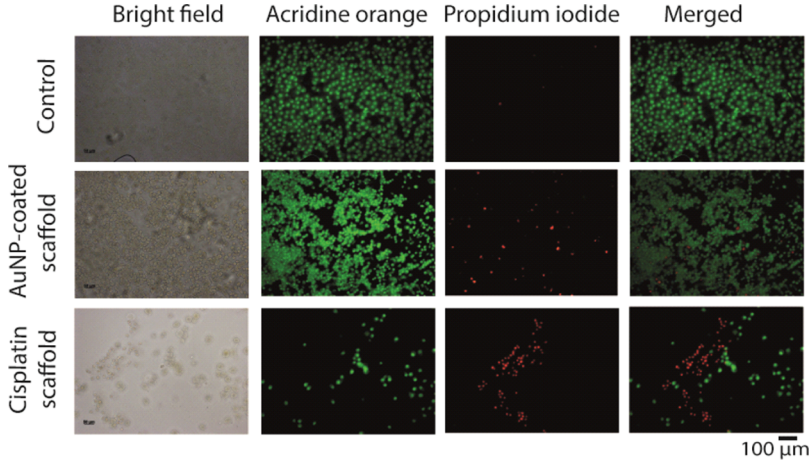

Figure 5. Live−dead assay by live-cell imaging. Live and dead cell stains are acridine orange and PI, respectively.

https://dx.doi.org/10.1021/acsomega.9b03694
ACS Omega 2020, 5, 20724−20733

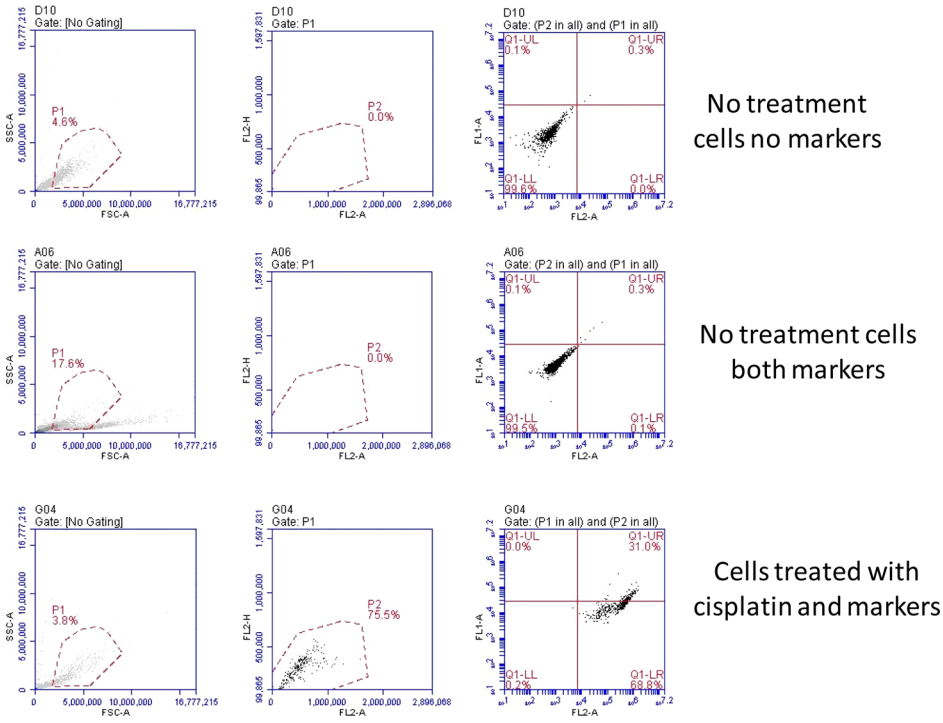

Figure 6. Flow cytometry analysis with cisplatin scaffold-exposed KB cells. Treatment time is 24 h. Fluorophores used were the Annexin V FITC conjugate for live-cell detection (in the FL2-A channel) and PI for dead cell detection (in the FL1-A channel). Every experiment was run in triplicates. Here, only the representative plots have been included.

membrane, indicating that cell apoptosis had progressed in a significant way.

Until this point, we have shown that drug-loaded scaffolds could release the drug in a slow, sustained manner and can cause cell death by cellular apoptosis. However, the uniqueness of the scaffolds that we prepared is their dual purpose. Therefore, post drug release, they are supposed to become cell-friendly to noncancerous new cells so that the intended volume filling can be accomplished. To probe this property, we conducted the following experiment using the L929 (murine fibroblast) cell line. A total of 5000 of these cells (L929) were seeded on the scaffolds from which the maximum amount of hydrated cisplatin was already released (48 h). The cell growth was followed by the resazurin assay. From the plot (Figure 7), it is evident that with time, the cellular population on scaffolds increased indicating the nontoxicity of the scaffolds after 2 days of cisplatin release. It may be noted that initially the growth of L929 cells is slow. We attribute this to the small amount of cisplatin that is still remaining anchored to the scaffold even after their incubation with the human mouth carcinoma cell line for 48 h. As cisplatin is highly cytotoxic, this small amount is sufficient to kill the L929 cells and this is what we see initially. Quite gratifyingly, the L929 cells proliferated considerably with time and came to a saturation point in 6 days (Figure 7). Thus, this steady increase in the viable cell population signifies the effectiveness of the drug-released scaffolds to maintain a healthy population of fibroblast cell lines. A TTEST was performed for the determination of the *P*-value, and the test results were incorporated in the data. The increased population of fibroblast cells was evident from the images (Figure 8) of the cellular population. Here, it can be clearly seen that at the beginning, only a few cells were able to attach to the scaffold. It may be also possible that at this stage after adhesion, cells (noncancerous) died because of leftover

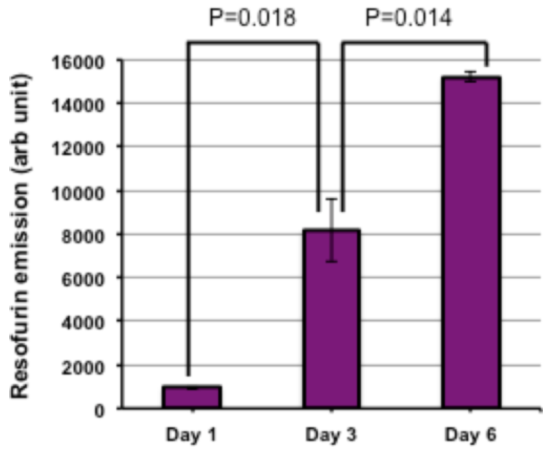

Figure 7. L929 cell growth on scaffolds after cisplatin release, where the quantification of cells was performed via mitochondrial activity using resazurin as an indicator (data are represented as the mean ± SD of $n = 3$).

cytotoxic drugs present. However, on each alternate day, as the media was changed, two effects can take place: (1) both dead cells and released drug molecules get eliminated and (2) existing cells received nutrients necessary for growth and proliferation. Ultimately, on day 6, cells formed a big colony, as shown in Figure 8. The quantification experiments clearly support this contention suggesting a tremendous improvement in cell population over 6 days (Supporting Information, Figure S10). Here, at this point, it is worth mentioning that the contact angle value (before and after drug release) did not change much (Supporting Information, Figure S11) and remained hydrophilic, a condition favorable for cell attachment and proliferation. We propose that the absence of drug and the

https://dx.doi.org/10.1021/acsomega.9b03694
ACS Omega 2020, 5, 20724−20733

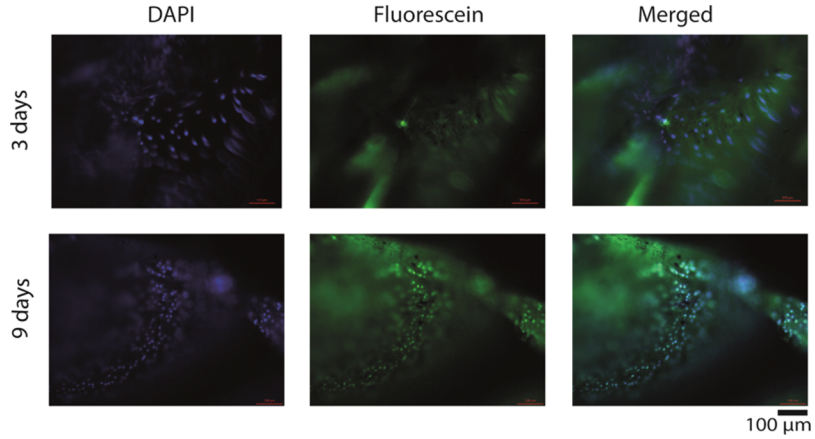

Figure 8. Representative fluorescence microscopy images showing L929 cell growth on scaffolds after cisplatin release. The nucleus and cytoplasm of L929 fibroblast cells were stained using DAPI and CFSE. The scale bar is 100 μm. Every experiment was performed in triplicates and several images were acquired. Only the representative images are being reported here.

retention of hydrophilicity (due to the presence of AuNPs) encouraged the cells to adhere and proliferate. Thus, the presented cisplatin-decorated scaffolds can release the cytotoxic drug during the first few days and hence can eliminate the remnant cancerous cells. Subsequent to the release of the drug, the cell-friendly surface chemistry of the scaffolds helps in the cell proliferation and to maintain a healthy cellular colony. This proves that the scaffold would be able to fulfill the role of a functional replacement in the real case.

CONCLUSIONS

In this report, we described the chemical conjugation of a cytotoxic drug cisplatin to porous solid scaffolds, which have been surface-modified by citrate-stabilized AuNPs. The scaffolds release the drug in a slow and sustained manner and then present a cell-friendly surface that can accept fresh cells in due course of time. The new cells form a colony (as proven by cell viability assay and cellular imaging), and thus, the scaffolds can act as a functional replacement hugely needed for the treatment of solid cancer. Although there have been several reports[28] of solid scaffolds working as drug cargo (local chemotherapy) and as a tissue engineering base independently, the relevant overlap of both these phenomena necessitates a surface modification strategy as described here where the scaffolds initially are highly cytotoxic before eventually becoming quite cell-friendly.

EXPERIMENTAL SECTION

Cisplatin, silver nitrate, *o*-phenylenediamine, PI, carboxyfluoresceinsuccinimidyl ester (CFSE), 4′,6-diamidino-2-phenylindole (DAPI), resazurin, PBS powder, and N-(2-hydroxyethyl)piperazine-N′-ethanesulfonic acid (HEPES) powder were bought from Sigma-Aldrich. The Annexin-V FITC conjugate was bought from Life Technologies. The human oral carcinoma originated KB cell line and murine fibroblast L929 cell line were procured from the animal cell repository maintained by NCCS, Pune, India. Dulbecco's modified Eagle's medium (DMEM) (low pyruvate) media and FBS were purchased from Invitrogen.

Preparation of Scaffolds. Porous HDPE scaffolds were cut into 4 mm diameter circular discs with 1 mm height. These were plasma-treated using N_2 + H_2 plasma at 80 W power for 20 min using Emitech Plasma Asher K1050X [Scheme 1A to B]. The scaffolds were immediately dipped and stirred in citrate-stabilized gold sol (water dispersion) prepared following the Turkevich method [Scheme 1B to C].[29] After overnight stirring on a magnetic stirrer, gold sol was found to lose the wine red color while a fine layer of AuNPs got attached to the plasma-treated HDPE scaffold. Gold sol was replenished and the stirring continued until no more AuNPs were getting deposited on the scaffold as concluded by the absence of any change in the color intensity of the gold sol.

Cisplatin powder (10 mg, 0.033 mmol) was taken in 10 mL of Milli-Q water. A total of 11.22 mg (2 equiv, 0.066 mmol) of silver nitrate was added to the suspension, which immediately formed a white precipitate (of AgCl). It was allowed to stir overnight. The reaction mixture was minicentrifuged for 10 min (at 12,500 rpm speed) and the supernatant was collected. It was filtered using a 0.22 μm syringe filter, which restricted the leftover AgCl to come into the filtrate. The concentration of cisplatin was assumed to be 1 mg/mL.

The water solution of aquated cisplatin was stirred overnight with AuNP-coated HDPE scaffolds at room temperature [Scheme 1C to D]. After 12 h of continuous agitation, the scaffolds were separated, washed with water, and dried in air and vacuum. Scaffolds thus got ready for characterization, followed by planned experiments in the tissue culture laboratory.

The cisplatin present on each scaffold was measured by the standard reaction with *o*-phenylenediamine[30] using a calibration curve (please see the Supporting Information sections S1 and S2).

Characterization. *Field Emission Scanning Electron Microscopy.* Field emission scanning electron microscopy (FESEM) imaging was performed using FESEM NNS450. For the pristine scaffold, gold-sputtering was performed before exposure to the electron beam. Other samples (which are already gold-coated) were used as it is.

X-ray Photoelectron Spectroscopy. The cisplatin-conjugated scaffolds were analyzed for the presence of platinum using XPS and ultraviolet photoelectron spectroscopy (UPS) on a Thermo Scientific-K-alpha+ instrument. The oxidation states of platinum atoms present on the scaffold surface were determined by deconvolution of the peaks.

https://dx.doi.org/10.1021/acsomega.9b03694
ACS Omega 2020, 5, 20724−20733

UV−Visible Spectroscopy. Solid-state UV−visible data were collected using a Shimadzu UV/Vis/IR/3600 spectrophotometer in the reflectance mode. For the background corrections, the barium sulfate standard was used. The polymer samples were frozen and powdered using a ball miller (Retsch Cryomill) before acquiring the data.

Micro-Scale X-ray Computed Tomography. Three-dimensional imaging of AuNP-coated HDPE scaffolds [Scheme 1C] was performed using an Xradia Versa 510 X-ray microscope (Zeiss X-ray microscope, Pleasanton, CA, USA). Scaffolds (4 mm diameter 1 mm height) were placed directly onto the sample holder, which was kept in between the X-ray source and detector assembly. The detector assembly consists of a scintillator, an objective lens, and a charge-coupled device camera. The X-ray source is ramped up to 80 kV and 7 W. The tomographic image acquisitions were completed by acquiring 3201 projections over 360° of rotation with a pixel size of 2.25 μm. Image processing software, Dragonfly Pro (Version 3.1), is used to generate a volume-rendered 3D image of scaffolds.

Cisplatin Calibration. In this method, 1.2 mg of *o*-phenylenediamine was weighed and taken in an Eppendorf tube. To it, 1.0 mL of dimethylformamide (DMF) and a known amount of (say 2 mg) cisplatin was added. It was sealed with Teflon tape heated at 100 °C for 2 h. The color changed to a shade of blue. The amount of cisplatin was varied (say 1.0, 0.5, 0.25, and 0.125 mg) in the same amount of ligand (1.2 mg *o*-phenylenediamine) and solvent (1 mL DMF). In UV spectrophotometry, the solution showed a peak at 706 nm. With a decrease or increase with the amount of cisplatin, the absorbance changed in a linear fashion. When the concentration versus absorbance was plotted, it produced a straight line (Figure S1).

Determination of Unknown Cisplatin. The same method as mentioned above was used for the determination of the amount of cisplatin present in a scaffold and for the analysis of release kinetics samples. For the determination of the amount of cisplatin present in one scaffold, a cisplatin-coated scaffold was dipped in 1.2 mg/mL *o*-phenylenediamine in DMF. It was sealed and heated at 100 °C for 2 h. The absorbance was determined using UV spectrophotometry. The concentration (hence the amount) of cisplatin present was backcalculated using the calibration curve, as shown in Section S1. Similarly, the amount of cisplatin present in each fraction of the release kinetics experiment was also calculated using the same protocol.

Cross-Checking the Role of Citric Acid Ligands in Conjugation with Hydrated Cisplatin Molecules. In this method, two sets of 4 mm diameter, 1 mm height porous HDPE discs (A in Scheme 1) and AuNP-coated HDPE discs (C in Scheme 1) were independently allowed to incubate in 1.0 mL of hydrated cisplatin sol (2.0 mg/mL) overnight. The following day, the scaffolds were removed, washed several times with fresh water, and dried and cisplatin estimation was performed following the regular protocol (Figure S2).

Expression of Phosphatidylserine by Annexin V Imaging. In this experiment, 50,000 healthy KB cells were seeded on coverslips placed inside each well of a 24-well plate. Drug-loaded scaffolds were placed inside wells. They were incubated for 1 and 2 days. At each time point, cells were washed with PBS and incubated in 5% bovine serum albumin (BSA) and 0.1% TritonX in PBS (0.5 mL each well) for 1 h. A total of 5 μL of Annexin V FITC was mixed with 195 μL of Annexin-binding buffer and added in the wells. After incubating the plate for 15 min in the dark at 0 °C, the cells were washed. Coverslips were placed upside down on clean glass slides. Live cells were observed using an Axio Observer Z1 Carl Zeiss microscope green filter.

Measurement of the Contact Angle before and after Release Kinetics. After in vitro release assay, the scaffolds (still coated with AuNPs) were separated, washed with water several times, and dried under vacuum. On these and cisplatin-carrying scaffolds (D in Scheme 1), a 10 μL water droplet was allowed to fall at room temperature and 1 atmospheric pressure from a certain height. Data were collected from a minimum of ∼5 locations and the average contact angle values were determined. Kruss Drop Shape Analyzer Version 1.41-02 was used for this purpose.

Release Kinetics Experiment. The drug release experiments were performed under sink conditions. For this, three porous HDPE scaffolds (each 4 mm diameter and 1 mm thickness, coated with AuNPs, and conjugated with cisplatin) were incubated in 10 mL of neutral PBS, as well as in the spent media (acidic) collected from the overgrown KB (human mouth carcinoma) cells. We ensured that the amount (10 mL) of solvents (PBS and spent media) taken was many folds higher than that required for the solubility of cisplatin in these respective solvents. A temperature of 37 °C (human body temperature) was maintained using a water bath, and the entire experiment was performed in triplicates. At definite time points, 100 μL of PBS or media (from the incubation mixture) was drawn out and evaporated to dryness using a speed vacuum concentrator/evaporator. After the sample withdrawal, 100 μL of PBS or media was also added to the original incubation chamber to avoid error because of a reduction in volume. The amount of cisplatin was colorimetrically determined by reacting with *o*-phenylenediamine as per the protocol described in the Supporting Information (see Sections S1 and S2) utilizing the already established calibration curve. The total amount of the drug released at each time point was calculated by multiplying the amount of cisplatin (μg) with a proper dilution factor. The percent release was calculated by normalizing with the average loading of cisplatin on each scaffold. Each experiment was carried out in triplicates and the standard error was incorporated while plotting.

$$\%\ \text{release} = \frac{\mu\text{g of Pt present at each time point}}{\text{average loading of Pt (in } \mu\text{g) on one scaffold} \times 3} \times 100$$

Cell Viability. The human mouth cancer cell line KB was maintained in 10% FBS/MEM complete media. In each well of a treated 12-well tissue culture plate, 50,000 healthy KB cells were seeded in 500 μL of complete MEM. It was allowed to incubate for 24 h in a 5% CO_2 atmosphere at 37 °C. Three wells were kept as the control. Untreated HDPE scaffolds, AuNP-coated scaffolds, cisplatin-coated scaffolds, and the equivalent amount of aquated cisplatin were added in each well in triplicates. At 48 h, the cells were incubated (6 h, 5% CO_2 atmosphere, 37 °C) with 100 μM resazurin in complete MEM. The emission at 590 nm was obtained by exciting the resofurin-containing media at 560 nm. While plotting, the emission from all the wells was normalized with the average emission of control cells (no treatment) and converted into percent. The result from each experiment was plotted as a mean including ±SE for n = 3.

https://dx.doi.org/10.1021/acsomega.9b03694
ACS Omega 2020, 5, 20724−20733

$$\%\ \text{cell viability} = \frac{\text{average emission from the cells exposed to drug-loaded scaffolds}}{\text{average emission from the control cells}} \times 100$$

A TTEST was performed for the determination of the P value and the test results were incorporated in the data.

Live−Dead Imaging Assay. In this assay, 50,000 healthy KB cells were seeded on the sterilized coverslips placed in each well of a 24-well plate. After overnight incubation, UV-sterilized citrate-capped AuNP-coated scaffolds and cisplatin−AuNP−HDPE scaffolds (3 of each type) were added 1 in number to each well. It was allowed to incubate overnight under cell culture conditions. Cells were washed with sterile PBS and incubated in 0.1% TritonX-100 and 5% BSA in PBS for 5.5 min in the dark. A total of 10 μL of 7.5 mM PI and 1 μL of 0.67 mM acridine orange in 1 mL of complete MEM media (for each well) were added and the cells were incubated under cell culture conditions for 1 h. The coverslips were washed with PBS, placed on clean slides upside down, and visualized under an Axio Observer Z1 Carl Zeiss microscope using green and red channels. Fluorescence emission was quantified using ZEN 2012 software and reported.

Flow Cytometry Analysis. In this assay, 10^6 human oral carcinoma KB cells were seeded in each well of a 6-well plate with 3 mL of complete media. After overnight incubation, drug (cisplatin)-loaded scaffolds and simple untreated scaffolds were added one in each well. Control wells were left blank. Again, after overnight incubation, cells were washed with sterile PBS and trypsinized with 1 mL of the trypsin−ethylenediaminetetraacetic acid mixture (for each well). Content from each well was diluted using 2 mL of PBS. Cells were collected in labeled falcon tubes (15 mL). Tubes were centrifuged at 1500 rpm for 3 min and aspirated. A total of 2 mL of PBS was added into each tube, the cell pellet was loosened (for washing) and centrifuged, and PBS was aspirated. To 6 tubes (one set of 3 tubes with the control scaffold and another set of 3 tubes with the cisplatin-containing scaffold), a cocktail of 5 μL of Annexin V FITC and 95 μL of Annexin-binding buffer was added. Another set of three tubes (control cells, without any scaffold) was kept as it is. The tubes were allowed to incubate in ice for 15 min in the dark. After the incubation, 2.0 mL of Annexin-binding buffer was added to each tube, centrifuged, and aspirated. To each of these 6 tubes, 50 μL of the PI reagent was added and incubated for 10 min in the dark. They were dispersed and filtered using a sterile strainer. Cells were directly analyzed for apoptosis using an Accuri C6 flow cytometry instrument. Data were compiled using the Accuri C6 software and are reported in Figure 6. Quantitative plotting is incorporated in Figure S6.

Annexin binding buffer preparation: Annexin binding buffer was prepared by mixing the following ingredients: 50 mL of dd-water, 0.4 gm of NaCl, 14 mg of $CaCl_2$, and 0.12 gm of HEPES.

PI reagent preparation: The PI reagent was prepared by mixing the following aliquots: 260 μL of 1 mg/mL PI stock, 600 μL of RNAse (6 μL RNAse from the stock), and 3 mL of Annexin binding buffer.

In the cytometer, the cells residing in live, early apoptotic, late apoptotic, and necrotic phases can be tracked by following the fluorescence intensity. In the data plot (Figure 6), the X-axis indicates green fluorescence and the Y-axis indicates red fluorescence. As a result, the first quadrant (bottom left) represents live cells, the bottom right quadrant represents early apoptotic cells (no dead cells yet but some are green), the top right quadrant represents late apoptotic cells (many cells are green), and finally, the top left quadrant represents necrotic cells.

Regrowth Experiment. After the release experiment (48 h time point), scaffolds were taken out, washed multiple times with PBS, and sterilized using UV light inside a biosafety cabinet. Each of the scaffolds was placed in each well of a sterile 96-well plate. L929 (murine fibroblast) cells were maintained using 10% FBS/DMEM media. To each well, 5000 number of L929 cells were added. As a control, the same number of cells was seeded on each well of an adherent 96-well plate. On each alternating day, media was changed. The experiment was followed by resazurin assay performed on each alternative day on the cells with scaffolds and control wells. The data from the scaffolds were normalized with the control adhering well data on the corresponding days, converted into percent, and plotted. A TTEST was performed for the determination of the P value and the test results were incorporated in the data.

Imaging of Regrown Cells. Another experiment exactly like the regrowth experiment was performed with the same number of L929 cells. The growth on scaffolds was monitored by microscopy using CFSE and DAPI as stains. The experimental procedure was similar to the regrowth experiment; only instead of the cell viability assay, at each time point, one scaffold was picked up using sterilized tweezers, fixed, permeabilized (using 5% BSA and 0.1% TritonX in PBS), and stained with DAPI and CFSE. Scaffolds were imaged using an Axio Observer Z1 Carl Zeiss microscope's green and blue filter. Images were quantified, normalized with respect to area, and plotted.

■ ASSOCIATED CONTENT

Supporting Information

The Supporting Information is available free of charge at https://pubs.acs.org/doi/10.1021/acsomega.9b03694.

Calibration curves for cisplatin determination, details of cisplatin determination, UV−vis spectra, 3D X-ray microtomography images, fluorescence quantification from cell images, fluorescence-activated cell sorting analysis, details of expression of phosphatidyl serine on cellular membrane, and contact angle measurements (PDF)

■ AUTHOR INFORMATION

Corresponding Author

Bhagavatula L. V. Prasad − *Physical/Materials Chemistry Division, National Chemical Laboratory (CSIR-NCL), Pashan, Pune 411008, India; Academy of Scientific and Innovative Research (AcSIR), Ghaziabad 201002, India;* orcid.org/0000-0002-3115-0736; Phone: 91-20-25902013; Email: pl.bhagavatula@ncl.res.in; Fax: 91-2025902636

Authors

Poulomi Sengupta − *Physical/Materials Chemistry Division, National Chemical Laboratory (CSIR-NCL), Pashan, Pune 411008, India; Academy of Scientific and Innovative Research (AcSIR), Ghaziabad 201002, India*

Vinay Agrawal − *Biopore Surgicals, Khar, Mumbai 400052, India*

https://dx.doi.org/10.1021/acsomega.9b03694
ACS Omega 2020, 5, 20724−20733

Complete contact information is available at:
https://pubs.acs.org/10.1021/acsomega.9b03694

Notes

The authors declare no competing financial interest.

■ ACKNOWLEDGMENTS

P.S. thanks DST-WOSA grant (grant number SR/WOS-A/CS-94/2012) for fellowship and financial support. P.S. also thanks AcSIR for Ph.D. registration. B.L.V.P. thanks CSIR, New Delhi, for the financial support through the M2D (CSC0134) project. The authors thank Aarti Yadav of CSIR-NCL for fitting the XPS data. We also thank Dr. D. Shanmugam Biochemistry Division, CSIR-NCL, for many useful discussions and suggestions.

■ REFERENCES

(1) Oral Cancer Diagnostics and Treatment Options. https://www.cancercenter.com/oral-cancer/types/tab/mouth-cancer/ (accessed January 2019).
(2) Shah, J. P.; Gil, Z. Current concepts in management of oral cancer − Surgery. *Oral Oncol.* **2009**, *45*, 394−401.
(3) Gupta, A.; Agrawal, G.; Tiwari, S.; Verma, K.; Agrawal, R.; Choudhary, V. Pectoralis major myocutaneous flap in head and neck reconstruction: an interesting experience from central India regional cancer center. *Int. Res. J. Med. Sci.* **2015**, *3*, 3065−3068.
(4) Treating Oral Cavity and Oropharyngeal Cancer. Cancer.org; American Cancer Society. https://www.cancer.org/cancer/oral-cavity-and-oropharyngeal-cancer/treating/surgery.html (accessed January 2020).
(5) Rai, A.; Datarkar, A.; Arora, A.; Adwani, D. G. Utility of High Density Porous Polyethylene Implants in Maxillofacial Surgery. *J. Maxillofac. Oral Surg.* **2014**, *13*, 42−46.
(6) Khan, F.; Tanaka, M. Designing smart biomaterials for tissue engineering. *Int. J. Mol. Sci.* **2018**, *19*, 17−31.
(7) Bružauskaitė, J.; Bironaitė, D.; Bagdonas, E.; Bernotienė, E. Scaffolds and cells for tissue regeneration: different scaffold pore sizes different cell effects. *Cytotechnology* **2016**, *68*, 355−369.
(8) Can, Z. Z.; Ercocen, A. R.; Apaydın, I.; Demirseren, E.; Sabuncuoglu, B. Tissue Engineering of high density porous polyethylene implant for three dimensional reconstruction: An experimental study. *Scand. J. Plast. ReConstr. Surg. Hand Surg.* **2000**, *34*, 9−14.
(9) James, S. P.; Oldinski, R.; Zhang, M.; Schwartz, H. *UHMWPE Biomaterials Handbook*, 2nd ed.; Elsevier, 2009; pp 259−276.
(10) Neovius, E.; Engstrand, T. Craniofacial reconstruction with bone and biomaterials: Review over the last 11 years. *J. Plast. Reconstr. Aesthetic Surg.* **2010**, *63*, 1615−1623.
(11) Deshpande, S.; Munoli, A. Long-term results of high-density porous polyethylene implants in facial skeletal augmentation: An Indian perspective. *Indian J. Plast. Surg.* **2010**, *43*, 034−039.
(12) Kim, Y. H.; Jang, T. Y. Porous high-density polyethylene in functional rhinoplasty: Excellent long-term aesthetic results and safety. *Plast. Surg.* **2014**, *22*, 14−17.
(13) Fernandez-Bueno, I.; Di Lauro, S.; Alvarez, I.; Lopez, J. C.; Garcia-Gutierrez, M. T.; Fernandez, I.; Larra, E.; Pastor, J. C. Safety and Biocompatibility of a New High-Density Polyethylene-Based Spherical Integrated Porous Orbital Implant: An Experimental Study in Rabbits. *J. Ophthalmol.* **2015**, *2015*, 1−7.
(14) Laquintana, V.; Trapani, A.; Denora, N.; Wang, F.; Gallo, J. M.; Trapani, G. New strategies to deliver anticancer drugs to brain tumors. *Expet Opin. Drug Deliv.* **2009**, *6*, 1017−1032.
(15) D'Britto, V.; Tiwari, S.; Purohit, V.; Wadgaonkar, P. P.; Bhoraskar, S. V.; Bhonde, R. R.; Prasad, B. L. V. Composites of plasma treated poly(etherimide) films with gold nanoparticles and lysine through layer by layer assembly: a "friendly-rough" surface for cell adhesion and proliferation for tissue engineering applications. *J. Mater. Chem.* **2009**, *19*, 544−550.
(16) Vermorken, J. B.; Remenar, E.; van Herpen, C.; Gorlia, T.; Mesia, R.; Degardin, M.; Stewart, J. S.; Jelic, S.; Betka, J.; Preiss, J. H.; van den Weyngaert, D.; Awada, A.; Cupissol, D.; Kienzer, H. R.; Rey, A.; Desaunois, I.; Bernier, J.; Lefebvre, J.-L. Cisplatin, Fluorouracil, and Docetaxel in Unresectable Head and Neck Cancer. *N. Engl. J. Med.* **2007**, *357*, 1695−1704.
(17) Cisplatin Side Effects. https://www.drugs.com/sfx/cisplatin-side-effects.html. (accessed January 2020).
(18) Blanchard, E. M. A study of the nucleation and growth processes in the synthesis of colloidal gold. *J. Solid Tumors* **2012**, *2*, 26−33.
(19) Sengupta, P.; Surwase, S. S.; Prasad, B. L. Modification of porous polyethylene scaffolds for cell attachment and proliferation. *Int. J. Nanomed.* **2018**, *13*, 87−90.
(20) Sengupta, P.; Prasad, B. L. V. Surface Modification of Polymeric Scaffolds for Tissue Engineering Applications. *Regen. Eng. Transl. Med.* **2018**, *4*, 75−91.
(21) Sengupta, P.; Prasad, B. L. V. Surface Modification of Polymers for Tissue Engineering Applications: Arginine Acts as a Sticky Protein Equivalent for Viable Cell Accommodation. *ACS Omega* **2018**, *3*, 4242−4251.
(22) Mulvaney, P. Surface Plasmon Spectroscopy of Nanosized Metal Particles. *Langmuir* **1996**, *12*, 788−800.
(23) Barnes, K. R.; Kutikov, A.; Lippard, S. J. Synthesis, characterization, and cytotoxicity of a series of estrogen-tethered platinum(IV) complexes. *Chem. Biol.* **2004**, *11*, 557−564.
(24) Dhar, S.; Gu, F. X.; Langer, R.; Farokhzad, O. C.; Lippard, S. J. Targeted delivery of cisplatin to prostate cancer cells by aptamer functionalized Pt(IV) prodrug-PLGA−PEG nanoparticles. *Proc. Natl. Acad. Sci. U.S.A.* **2008**, *105*, 17356−17361.
(25) Shen, D.-W.; Pouliot, L. M.; Hall, M. D.; Gottesman, M. M.; Gottesman, M. M. Cisplatin Resistance: A Cellular Self-Defense Mechanism Resulting from Multiple Epigenetic and Genetic Changes. *Pharmacol. Rev.* **2012**, *64*, 706−721.
(26) Shen, D.-w.; Akiyama, S.-i.; Schoenlein, P.; Pastan, I.; Gottesman, M. Characterisation of high-level cisplatin-resistant cell lines established from a human hepatoma cell line and human KB adenocarcinoma cells: cross-resistance and protein changes. *Br. J. Cancer* **1995**, *71*, 676−683.
(27) Paraskar, A. S.; Soni, S.; Chin, K. T.; Chaudhuri, P.; Muto, K. W.; Berkowitz, J.; Handlogten, M. W.; Alves, N. J.; Bilgicer, B.; Dinulescu, D. M.; Mashelkar, R. A.; Sengupta, S. Harnessing structure-activity relationship to engineer a cisplatin nanoparticle for enhanced antitumor efficacy. *Proc. Natl. Acad. Sci. U.S.A.* **2010**, *107*, 12435−12440.
(28) Sharma, P. K.; Taneja, S.; Singh, Y. Hydrazone-Linkage-Based Self-Healing and Injectable Xanthan-Poly(ethylene glycol) Hydrogels for Controlled Drug Release and 3D Cell Culture. *ACS Appl. Mater. Interfaces* **2018**, *10*, 30936−30945.
(29) Turkevich, J.; Stevenson, P. C.; Hillier, J. A study of the nucleation and growth processes in the synthesis of colloidal gold. *Discuss. Faraday Soc.* **1951**, *11*, 55−75.
(30) Golla, E. D.; Ayres, G. H. Spectrophotometric determination of platinum with o-phenylenediamine. *Talanta* **1973**, *20*, 199−210.

https://dx.doi.org/10.1021/acsomega.9b03694
ACS Omega 2020, 5, 20724−20733